A Bio-Inspired Reservoir-Computer for Real-Time Stress Detection From ECG Signal

Sanjeev Tannirkulam Chandrasekaran, *Graduate Student Member, IEEE*, Sumukh Prashant Bhanushali, Imon Banerjee, and Arindam Sanyal, *Member, IEEE*

***Abstract*—This letter presents the first on-chip bio-inspired reservoir computer (RC) prototype implemented in a 65-nm CMOS. The RC comprises 50 time-multiplexed neurons, and each neuron embeds a strong nonlinearity in a feedback loop. The RC applies a nonlinear transformation to the input and projects it to high-dimensional space, thus allowing linear separation by a simple logistic-regression (LR) layer implemented off-chip. We demonstrate real-time stress detection from electrocardiogram (ECG) signals using the RC. The RC achieves 93% classification accuracy which is 6% better than the state-of-the-art digital classifiers. Operating at 40 kHz, the prototype consumes 27.5 nJ/classification which is 7× lower than the state-of-the-art ECG processors performing similar complexity classification task.**

***Index Terms*—Electrocardiogram (ECG) sensor, machine learning (ML), reservoir computing, stress detection.**

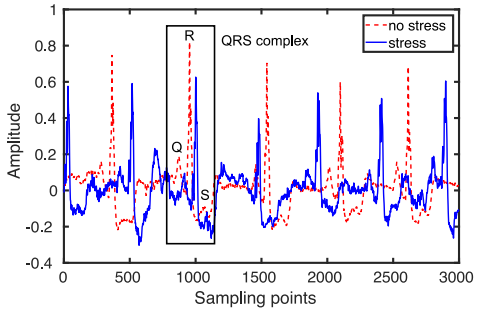

Fig. 1. Example ECG plots for stress and no-stress conditions.

I. Introduction

Stress activates the sympathetic nervous system (SNS) which in turn leads to physiological changes, such as change in electrical activity of the heart which can be detected through minimally intrusive electrocardiogram (ECG) sensor. Long-term stress in humans can cause several diseases ranging from musculoskeletal illness to cardiovascular disease. The severe side-effects of stress calls for real-time continuous stress detection to increase awareness of high stress levels which may otherwise go undetected. While advances in machine learning (ML) has created potential for automated monitoring of stress level from wearable ECG sensor, real-time continuous stress detection using ML has not been demonstrated so far. Instead, most existing works collect ECG data from sensor over a time-interval and analyze the sensor data offline using the digital ML model. This is likely because classification of temporal signals through conventional ML models are computationally intensive since these algorithms require computation of many input features and/or complex nonlinear projections which makes their integration on sensors challenging.

The contribution of this letter is to demonstrate an on-chip ML classifier that consumes only 27.5 nJ/classification while detecting stress from ECG signal with 93% accuracy. In contrast, an on-chip ML classifier with similar classification complexity [1] consumes 186 nJ/classification which is 7× higher than that of our classifier. To reduce energy of the proposed classifier, we adopt two design techniques: 1) use time-domain (TD) features for classification and 2) use reservoir computing architecture that mimics highly energy efficient computation ability of the brain cortex. The feature extraction technique and reservoir computing architecture are described in Sections II and III, respectively. The circuit design is discussed in Section IV, measurement results on a 65-nm CMOS prototype and comparison with other works are presented in Section V.

Manuscript received May 18, 2020; revised July 28, 2020; accepted August 11, 2020. Date of publication August 17, 2020; date of current version September 3, 2020. This article was approved by Associate Editor Paul Walsh. This work was supported by the Air Force Research Laboratory under Agreement FA8650-18-2-5402. *(Corresponding author: Sanjeev Tannirkulam Chandrasekaran.)*

Sanjeev Tannirkulam Chandrasekaran, Sumukh Prashant Bhanushali, and Arindam Sanyal are with the Department of Electrical Engineering, University at Buffalo, Buffalo, NY 14260 USA (e-mail: stannirk@buffalo.edu).

Imon Banerjee is with the Department of Biomedical Informatics, Emory University, Atlanta, GA 30322 USA.

Digital Object Identifier 10.1109/LSSC.2020.3016924

II. Stress Dataset and Feature Extraction

We used the WESAD dataset [2] for demonstrating the proposed classifier. The WESAD dataset contains multimodal, physiological sensor data of 15 patients collected from wrist and chest at 700-Hz sampling rate. The sensor data for each patient is recorded for approximately 2 h out of which the patient was under stress for roughly 10 min. The sensor data is annotated as baseline, stress, amusement, or meditation conditions. For this letter, we used ECG signal from the chest and performed binary stress versus nonstress classification. Fig. 1 shows an example ECG plot from the WESAD dataset for stress and no-stress conditions.

To unskew the training data, we created 1020 3-min overlapping segments of the sensor data such that number of segments with stress are roughly equal to number segments without stress. Each segment has an overlap of 6.6 s with the following segment. Out of 1020 segments, 525 segments are from "stress" class, while the remaining 495 segments are from "no-stress" class.

We use TD features for classifying stress in contrast to using frequency-domain (FD) or combination of time- and frequency-domain features. TD features are based on first-order statistics, such as mean, standard deviation, etc., which are much less computationally intensive than FD features. The TD features used in this letter are derived following statistical measures of heart-rate variability (HRV) presented in [3] and are calculated on normal-to-normal (NN) intervals which are intervals between adjacent QRS complexes (see Fig. 1) in the ECG signal. The NN intervals are calculated from distances between peaks in the ECG signal. The TD features used in this letter are summarized in Table I and are calculated from 3-min segments of ECG signal which allows comparison of HRV during stress and nonstress conditions. Synthesized in 65-nm CMOS process from Verilog RTL descriptions, the TD feature extractor consumes

TABLE I
SUMMARY OF TIME-DOMAIN FEATURES

SDNN	The standard deviation of all NN intervals
RMSSD	The square root of the mean squared differences of successive NN intervals
NN50	The number of interval differences of successive NN intervals greater than 50 ms
PNN50	The proportion derived by dividing NN50 by the total number of NN intervals
SDSD	The standard deviation of differences between adjacent NN intervals

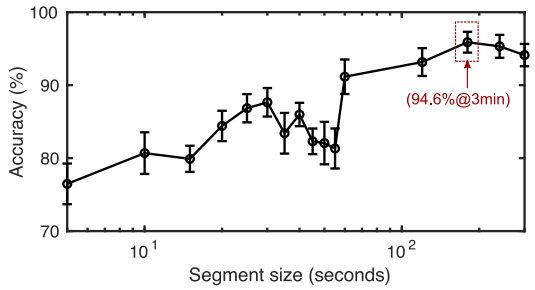

Fig. 2. Simulated classification accuracy versus segment size.

6× lower power and 900× smaller area than FD feature extractor. We used the FD features reported in [2] for comparison. Fig. 2 shows the simulated classification accuracy versus segment size. For each segment size, the simulation is repeated 50 times by randomly partitioning the data into the training and test sets. The highest mean accuracy is obtained for 3-min segment size.

III. RESERVOIR COMPUTING

Reservoir computing is a branch of ML that uses random, nonlinear projection of inputs to high-dimensional space to improve separability of distinct signals in the input. A reservoir computer (RC) uses a network of generic neurons with random connections to mimic the recurrent looping structure in the cortex. The input weights as well as the sparse connection matrix inside the reservoir are generated randomly while the output layer consists of a memory-less, linear read-out with trainable weights. The simple architecture of reservoir computing reduces computation and makes it attractive for sensor integration compared to more conventional ML algorithms.

Fig. 3 shows the architecture of our RC for a temporal input $X[n]$. The input is multiplied with a weight matrix W and passed through reservoir nonlinearity to an N-dimensional reservoir space $r[n]$, where N is the number of neurons in the reservoir. The weight matrix, W, has a dimension of $N \times 1$. The reservoir output can be mathematically written as [4]

$$r[n] = H\big(G_i W \times \vec{X}[n] + G_f W_r \times r[n-1]\big) \tag{1}$$

where $H(\cdot)$ is the reservoir nonlinearity function, W_r is the $N \times N$ reservoir connectivity matrix, and G_i and G_f are input and feedback scaling factors. W_r is an identity matrix while elements of W are randomly set to "0" or "1" which reduces the weight multipliers in Fig. 3 by switches. The sparsely filled connectivity matrix W_r provides memory to the reservoir to handle temporal structure in the input data. The reservoir outputs are then combined and passed to the output layer for classification. We use a logistic-regression (LR) classifier as the output layer such that the overall classifier output is given by $d[n] = 1/(1 + \exp(-W_o^T \times r[n]))$ where W_o is the $N \times 1$ output weight matrix.

Fig. 4(a) shows the circuit schematic for the proposed reservoir computing architecture shown in Fig. 3. The feature extraction and

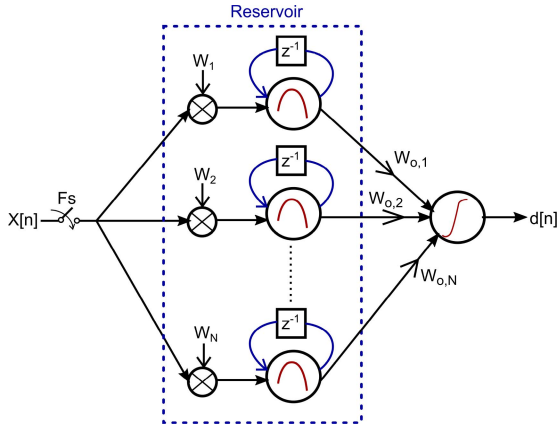

Fig. 3. Proposed reservoir computing architecture.

output layer are implemented digitally off-chip. The number of neurons in the reservoir, N, is set to 50. We use a 10-bit successive approximation register (SAR) ADC to quantize the reservoir states. To save area, we time-multiplex the reservoir computing ML (RCML) classifier as shown in Fig. 4(b). The inputs are sampled at the same sampling frequency F_s as in Fig. 4(a), but the feedback loop operates at $N \times F_s = 2$ MHz.

Computations in the reservoir are performed in the mixed-signal domain which eliminates memory access associated with storing intermediate results. Only the output layer is trained and requires storage for the trained weights. Thus, computation and storage requirements are significantly relaxed compared to traditional ML circuits with multiple layers all of which performs many computations in digital domain and requires storage for trained weights and intermediate results. Compared to linear discriminant analysis (LDA) and random forest (RF) classifiers [2], the proposed RCML classifier requires 20× and 110× lower memory, respectively, while having higher accuracy.

IV. CIRCUIT DESIGN

An OTA is used to implement the summation in (1) and a resistive DAC is used for the feedback. We use indirect Miller-compensated two-stage amplifier with 60-dB gain for the OTA. A common-source amplifier with resistive feedback is used to implement nonlinearity in the reservoir neurons. Transfer function of the nonlinearity is shown in Fig. 4(b) and is inspired by nonlinearity term in Mackey-Glass equation [5] which can efficiently model behavior of different physiological systems. Output of the nonlinearity circuit is fed to a unity-gain buffer which drives 2.4-pF capacitive DAC of the 10-bit SAR ADC.

The reservoir should have an optimum sensitivity to adequately separate inputs from different classes but not generate significantly different response to inputs from the same class. The reservoir sensitivity is controlled by the DAC gain, G_f. Fig. 5(a) shows the simulated classification accuracy as a function of DAC gain. The reservoir becomes unstable for DAC gain greater than 0.6. The DAC gain is set to 0.4 for this letter. In addition to having good sensitivity, noise in the reservoir should be low to ensure that reservoir states are repeatable. The DAC, OTA-adder, nonlinearity, and unity-gain buffer contribute to 0.3 mV, rms noise at noise bandwidth of 130 MHz when referred to the ADC input, while the 10-b ADC has an input-referred noise of 0.54 mV, rms. Fig. 5(b) shows simulated classification accuracy versus ADC resolution. A 10-b ADC resolution is selected for this design to ensure good classification accuracy. Fig. 5(c) shows the measured

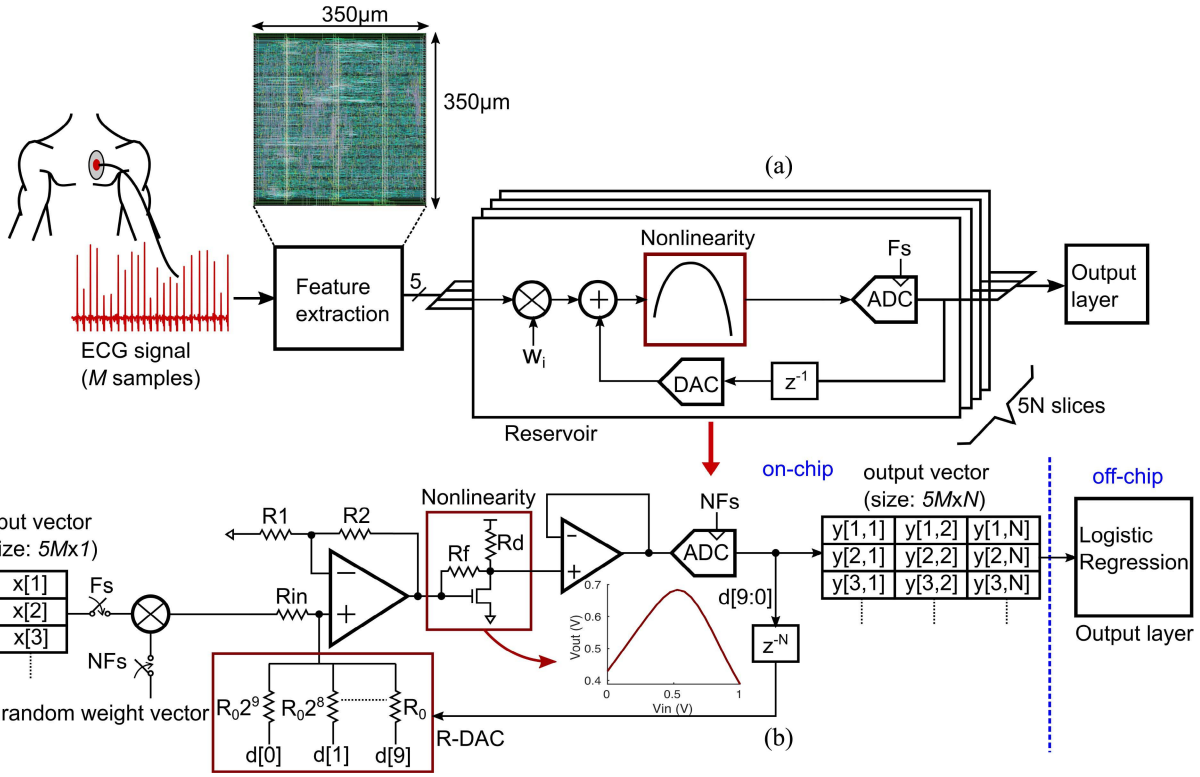

Fig. 4. (a) Circuit schematic of the proposed unrolled RCML. (b) Time-multiplexed RCML circuit.

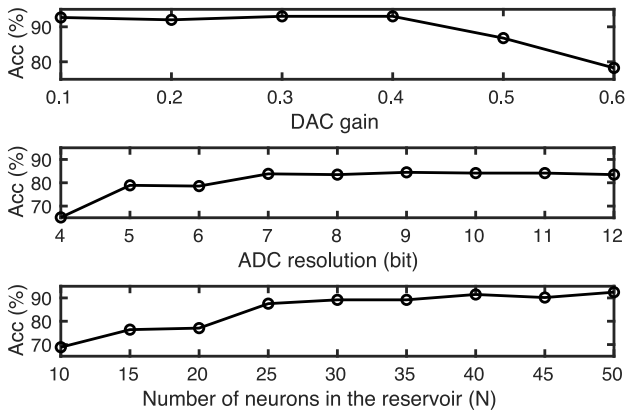

Fig. 5. Simulated classification accuracy versus (a) DAC gain, (b) ADC resolution, and measured accuracy versus N.

TABLE II
ACCURACY AS A FUNCTION OF SELECTED FEATURES

	SDNN	RMMSD	NN50	PNN50	SDSD	NN50+PNN50 +SDNN
Acc(%)	69	61	75	78	62	89

classification accuracy versus number of reservoir neurons, N. The classification accuracy exceeds 90% for $N > 35$.

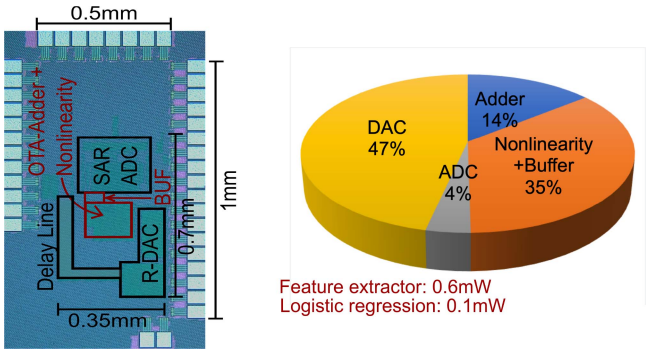

Fig. 6. Die photograph and power breakdown of RCML classifier.

Fig. 7. Measured confusion matrix for test dataset.

V. MEASUREMENT RESULTS

Fig. 6 shows the die microphotograph of the proposed RCML classifier in a 65-nm CMOS process and power breakdown. The on-chip classifier consumes 0.4 mW from 1.2-V supply. The R-DAC consumes 47% of the classifier power, while the nonlinearity and unity-gain buffer consume 35% of the classifier power. The feature extractor and output LR blocks are synthesized in 65-nm CMOS process and consume 0.6 mW and 0.1 mW, respectively. While our chip measurements are performed at accelerated time scale, the power consumption can be significantly reduced for real application if the chip operates at 6.6 s which is the overlap

TABLE III
COMPARISON WITH ML CLASSIFIERS FOR STRESS DETECTION

	Classifier	Feature	Accuracy(%)
[2] ICMI'18	LDA	TD+FD	85
[8] ACII'13	k-NN	TD	87
[9] ACII'13	SVM	TD+FD	72
[10] TAC'16	SVM	TD+FD	78
This work	**RCML+LR**	**TD**	**93**

TABLE IV
COMPARISON WITH ECG PROCESSOR ASICS

	Process (nm)	Freq. (kHz)	Energy
[1] JSSC'14	90	0.27	186nJ
[11] JBHI'14	180	0.1	504nJ
[6] VLSI'10	180	1	4.2μJ
[7] JSSC'13	130	1500	124μJ
This work	**65**	**40**	**27.5nJ**

interval between adjacent frames. By adopting switched-capacitor architecture for the OTA-adder and DAC, the power of the chip can be scaled in proportion to the operating frequency and will be limited by leakage power at very low frequencies. The leakage power for our chip is 34 nW. If the proposed RCML classifier is implemented digitally on an embedded system, such as Arm Cortex-M3 with 65-nm processor, the fully digital classifier will require 2978 instructions and consume 21.6× more power than our prototype.

Out of 1020 patient data, the RCML classifier is trained with 715 patient ECG data and tested with 305 patient ECG data with features calculated over 3-min windows. Fig. 7 shows the measured confusion matrix for test dataset. The classifier has accuracy of 93%, specificity of 88.6% and a high sensitivity of 95.3% which is important for clinical decision making. If the ECG data is directly sent through an LR network instead of first going through nonlinear projection by our reservoir, the classification accuracy on the test dataset drops to 75%. Table II shows the measured accuracy for selected features. If only one feature is considered for classification, the highest accuracy of 78% is obtained with PNN50, while the accuracy improves to 89% if the top 3 features with highest individual accuracies are used for classification. Thus, even though all the features are derived from the same NN intervals, all five features are required to reach 93% accuracy.

Table III compares the performance of the proposed RCML classifier with existing works on stress detection from physiological sensor signals. The ML classifiers reported in Table III, except for our work, are all implemented in software and use both TD and TD+FD features. Our RCML classifier has the highest accuracy of 93% which is 6% better than state-of-the-art. Table IV compares our ECG classifier with the state-of-the-art ECG processors which are all implemented in digital domain and use conventional ML algorithms, like SVM. The works in [1], [6], and [7] derive HRV related features from ECG signals to predict arrhythmia, which has similar classification complexity as stress detection. The proposed RCML classifier has the lowest energy consumption thanks to the mixed-signal reservoir architecture and TD features.

ACKNOWLEDGMENT

The U.S. Government is authorized to reproduce and distribute reprints for Government purposes notwithstanding any copyright notation thereon. The views and conclusions contained herein are those of the authors and should not be interpreted as necessarily representing the official policies or endorsements, either expressed or implied, of Air Force Research Laboratory or the U.S. Government.

REFERENCES

[1] S.-Y. Hsu, Y. Ho, P.-Y. Chang, C. Su, and C.-Y. Lee, "A 48.6-to-105.2 μW machine learning assisted cardiac sensor SoC for mobile healthcare applications," *IEEE J. Solid-State Circuits*, vol. 49, no. 4, pp. 801–811, Apr. 2014.

[2] P. Schmidt, A. Reiss, R. Duerichen, C. Marberger, and K. Van Laerhoven, "Introducing WESAD, a multimodal dataset for wearable stress and affect detection," in *Proc. 20th ACM Int. Conf. Multimodal Interact.*, 2018, pp. 400–408.

[3] A. J. Camm *et al.*, "Heart rate variability: Standards of measurement, physiological interpretation and clinical use.Task force of the European society of cardiology and the North American society of pacing and electrophysiology," *Circulation*, vol. 93, no. 5, pp. 1043–1065, 1996.

[4] S. Ortín *et al.*, "A unified framework for reservoir computing and extreme learning machines based on a single time-delayed neuron," *Sci. Rep.*, vol. 5, Oct. 2015, Art. no. 14945.

[5] A. Namajünas, K. Pyragas, and A. Tamaševičius, "An electronic analog of the Mackey-Glass system," *Phys. Lett. A*, vol. 201, no. 1, pp. 42–46, 1995.

[6] H. Kim, R. F. Yazicioglu, T. Torfs, P. Merken, H.-J. Yoo, and C. V. Hoof, "A low power ECG signal processor for ambulatory arrhythmia monitoring system," in *Proc. IEEE Symp. VLSI Circuits*, Honolulu, HI, USA 2010, pp. 19–20.

[7] K. H. Lee and N. Verma, "A low-power processor with configurable embedded machine-learning accelerators for high-order and adaptive analysis of medical-sensor signals," *IEEE J. Solid-State Circuits*, vol. 48, no. 7, pp. 1625–1637, Jul. 2013.

[8] A. Sano and R. W. Picard, "Stress recognition using wearable sensors and mobile phones," in *Proc. IEEE Hum. Assoc. Conf. Affect. Comput. Intell. Interact.*, Geneva, Switzerland, 2013, pp. 671–676.

[9] M. Soury and L. Devillers, "Stress detection from audio on multiple window analysis size in a public speaking task," in *Proc. Hum. Assoc. Conf. Affect. Comput. Intell. Interact.*, Geneva, Switzerland, 2013, pp. 529–533.

[10] J. Aigrain, M. Spodenkiewicz, S. Dubuisson, M. Detyniecki, D. Cohen, and M. Chetouani, "Multimodal stress detection from multiple assessments," *IEEE Trans. Affect. Comput.*, vol. 9, no. 4, pp. 491–506, Oct.–Dec. 2018.

[11] S.-Y. Lee, J.-H. Hong, C.-H. Hsieh, M.-C. Liang, S.-Y. C. Chien, and K.-H. Lin, "Low-power wireless ECG acquisition and classification system for body sensor networks," *IEEE J. Biomed. Health Inform.*, vol. 19, no. 1, pp. 236–246, Jan. 2015.